2024 European Control Conference (ECC)
June 25-28, 2024. Stockholm, Sweden

Distributed two-layer predictive control of multi-energy systems

Lorenzo Nigro[1,2], Alessio La Bella[1] and Riccardo Scattolini[1].

Abstract— **Multi-energy systems (MESs) involve the synergetic operation of different energy vectors, unlocking higher system flexibility and efficiency. Nonetheless, they suffer from high model complexity, large-scale dimension, and different dynamical transient time constants. Moreover, each energy vector may have its own stakeholder, raising privacy concerns. In this framework, this article proposes a distributed two-layer predictive control architecture enabling to solve the mentioned issues. The lower level consists of decentralized Model Predictive Control (MPC) regulators considering detailed models, possibly nonlinear, while the high level exploits a convex and unified energy modelling of each energy vector using a fully distributed algorithm named Dual Consensus ADMM (DC-ADMM). The proposed control architecture is tested on an extended case study composed of three interconnected energy vectors i.e., a hydrogen energy system, a district heating network from the literature, and the IEEE 37-bus power system, showing promising results.**

I. Introduction

Multi-energy systems (MESs) are a possible solution for the decarbonization of energy system. MES consists of the synergetic operation of different energy vectors together, unlocking higher system flexibility and efficiency [1]. They achieve these benefits through meaningful energy exchange among different energy vectors, e.g., electrical, gas, or district heating networks. The energy exchanges is enabled by interface devices availability e.g., heat pumps (electrical-to-thermal energy), fuel cells (gas-to-electrical energy) or boilers (gas-to-thermal energy). Nonetheless, the control of MES is not an easy task due to the model complexity, the large-scale dimension, and the time constants diversity, e.g., fast electrical dynamics and slow thermal ones. Also, the control approach should deal with privacy concerns as the subsystems may belong to different system operators.

Recently, the literature worked on finding appropriate control architectures for multi-energy systems [2]. A common reference model is the *energy hub* (EH), a linear and lumped-element framework to develop new control techniques for MES [3], e.g., optimal control through model predictive control (MPC) [4]. Increasing control complexity, mixed-integer linear models [5], time-varying constraints [6] or data-driven methods [7], [8] are present in the literature. Unfortunately, these solutions are based on centralized controls which suffer from scalability issues (i.e., computational problems related to agents number or complexity growth) due to energy vector models' complexity, and they do not preserve local confidential information. This complexity led others to test hierarchical control strategies [9], [10] pushing the complexity to lower levels trying to achieve lightweight centralized high level optimization problems. Nonetheless, scalability issues also affects pure hierarchical approaches. Distributed control approaches may solve scalability and privacy issues, but their optimality, convergence and feasibility are guaranteed only in the presence of convexity [11]. Though, MES are typically characterized by nonconvex and nonlinear models. Thus, some distributed approaches present in the literature exploit either linear problems or MILP formulations resulting in simplified models that are less optimal in energy vector management, e.g., due to the inability to utilize networks effects [12], [13].

Given the above discussion, the main goal of this work is to propose a control architecture that solves scalability and privacy concerns and exploits the benefits of distributed algorithms in the presence of nonlinear models to optimally coordinate MES. This is possible thanks to a novel modelling technique that exploits low level data to create a high level problem that is convex and unified across all energy vectors.

The proposed control strategy is based on a distributed two-layer architecture. The lower level consists of several local decentralized MPC, each one controlling an energy vector with a suitable time-rate and nonlinear model. The local MPC minimizes the local operational costs, while tracking references on the total energy to be stored and on the power exchanges among different vectors imposed by the high-level layer. The latter is based on a distributed framework of supervising MPC regulators, exploiting the Dual Consensus ADMM algorithm [11], a fully distributed scheme with enhanced scalability properties [14]. Additionally, we guarantee the distributed algorithm convergence by exploiting the generalized energy formulation previously developed in [10]. This modelling technique unlocks a unified convex representation of different energy vectors and ensures distributed control strategies convergency.

We analyze the proposed control architecture performances on an extended MES example composed of three energy vectors: a gas network, a district heating network, the AROMA [15], and a power system, the IEEE 37bus. The collected data support the proposed control optimality and scalability. The work is an evolution of [10], surpassing its shortcomings in two ways: getting rid of the high-level centralized layer and its scalability and privacy-related issues, and ensuring that power exchanges among multi-energy subsystems are locally imposed by the local regulators instead of being imposed by a supervisory layer.

[1]Alessio La Bella, Lorenzo Nigro and Riccardo Scattolini are with the Dipartimento di Elettronica, Informazione e Bioingegneria, Politecnico di Milano, 20133 Milan, Italy (alessio.labella@polimi.it, lorenzo.nigro@polimi.it and riccardo.scattolini@polimi.it)

[2]Lorenzo Nigro with RSE S.p.A. - Research on Energy System, Milan 20134, MI, Italy.

Notation: We denote the set of real numbers as $\mathbb{R}$. Moreover, given a matrix A, $A \in \mathbb{R}^{n,\,m}$ represents a real-valued matrix with n rows and m columns. Considering the same matrix, we indicate as A' its transpose. The operator $blkdiag(\{A\}_n)$ defines a block-diagonal matrix with n-times matrix A as blocks. The same holds for vectors. We denote as $\mathbb{1}$ a 1D vector of suitable dimensions which entries are all 1, e.g., $[1, \ldots, 1]'$. The same holds for the vector $\mathbb{0}$ which entries equal to 0. Furthermore, the lower and upper bounds of a vector $x \in \mathbb{R}^n$ are $\underline{x} \in \mathbb{R}^n$ and $\bar{x} \in \mathbb{R}^n$ respectively, it holds $\underline{x} < \bar{x}$. Finally, given a set of indexes $\mathcal{N} = \{1, \ldots, n\}$ with cardinality $card(\mathcal{N})$ and a related sequence of variables $s_1, \ldots, s_n$, the vectors $s^\dagger = [s_1, \ldots, s_n]'$ is written element-wise as $s^\dagger = \{s_i\}_{\forall i \in \mathcal{N}}$.

II. Problem statement

Define a multi-energy system $\mathcal{S}^\dagger$ including M subsystems $\mathcal{S}_1, \ldots, \mathcal{S}_M$. The generic $\mathcal{S}_i$ consists of a specific energy vector with its own generators, loads and storage units, e.g., a subsystem $\mathcal{S}_i$ can represent an electrical grid or a district heating network. Subsystems may be able to exchange power among each other through power interfaces which allow the overall MES $\mathcal{S}^\dagger$ management optimization. Example of these interfaces are fuel cells for gas-to-electrical or heat pumps for electrical-to-thermal energy. It is possible to formalize MES structure using a directed graph $\mathcal{G} = (\mathcal{N}, \mathcal{E})$, where $\mathcal{N} = \{1, \ldots, M\}$ identifies the set of subsystems, while $\mathcal{E}$ denotes the edges' set modelling the interconnections among subsystems, i.e., $(i, j) \in \mathcal{E}$ if the power p_{ij}^{tr} can be transferred between $\mathcal{S}_i$ and $\mathcal{S}_j$. As a convention, in the following assume the transferred power p_{ij}^{tr} positive if flowing according to the edge's orientation, i.e., if transferred from $\mathcal{S}_i$ to $\mathcal{S}_j$ with $(i, j) \in \mathcal{E}$. For each node $i \in \mathcal{N}$, the connected nodes set is $\mathcal{N}_i = \{j \in \mathcal{N} | (i,\, j) \vee (j,\, i) \in \mathcal{E}\}$ regardless of the edge orientation, with $n_i = card(\mathcal{N}_i)$.

Each subsystem $\mathcal{S}_i$ can be modelled as a nonlinear system

$$\dot{x}_i(t) = f_i^s(x_i(t), u_i(t), \tilde{d}_i(t)), \tag{1a}$$

where $x_i \in \mathbb{R}^{x_i}$ represents the local states vector and $u_i \in \mathbb{R}^{m_i}$ is the input vector, locally bounded as

$$\underline{x}_i \leq x_i(t) \leq \bar{x}_i, \tag{1b}$$

$$\underline{u}_i \leq u_i(t) \leq \bar{u}_i. \tag{1c}$$

Furthermore, the exogenous signal vector $\tilde{d}_i(t)$ in (1a) is

$$\tilde{d}_i(t) = [d_i(t)'\, w_i(t)']', \tag{1d}$$

where $d_i(t) \in \mathbb{R}^{r_i}$ are the local disturbances of $\mathcal{S}_i$, while w_i is the vector of power exchanges of $\mathcal{S}_i$ with other connected subsystems. Specifically,

$$w_i(t) = \{p_{ij}^{tr}(t)\}_{j \in \mathcal{N}_i} \tag{1e}$$

where $w_i(t) \in \mathbb{R}^{n_i}$. Additionally, each subsystem $\mathcal{S}_i$ includes g_i controllable sources and l_i nondispatchable units. Hence, each $\mathcal{S}_i$ controllable power generation is $p_i^g \in \mathbb{R}^{g_i}$ and the nondispatchable power is $p_i^l \in \mathbb{R}^{l_i}$, and they have the following expressions

$$p_i^g(t) = \phi_i(x_i(t),\, u_i(t)), \tag{1f}$$

$$p_i^l(t) = \psi_i(x_i(t),\, d_i(t)). \tag{1g}$$

Specifically, the power produced by controllable sources depends on local states and inputs, whereas the noncontrollable power depends on local states and external disturbances. For the sake of clarity, nondispatchable units relate to either loads or nondispatchable generators, e.g., renewable energy sources.

The subsystems' models (1) can be nonlinear, nonconvex, and large-scale dimension (e.g., if $\mathcal{S}_i$ is a thermal energy network). Thus, it is not suited for efficient MES optimization as its implementation in centralized control approaches would suffer from computational and scalability issues, while fully distributed architectures would present convergence and feasibility problems. Hence, a high-level subsystem's reduced energy modelling is introduced and discussed in details in [10]. This model enables the design of a novel distributed multi-layer control architecture. The formulation represents each $\mathcal{S}_i$ with an energy based model independent of the specific energy vector.

Assumption 1: Consider the i-th subsystem represented as (1), its total stored energy is

$$e_i = \xi_i(x_i), \tag{2}$$

where $e_i \in \mathbb{R}$ and $\xi_i : \mathbb{R}^{n_i} \to \mathbb{R}$. Also, the stored energy dynamic is

$$\dot{e}_i(t) = \mathbb{1}'_{g_i} p_i^g(t) - \mathbb{1}'_{l_i} p_i^l(t) - \mathbb{1}'_{n_i} w_i(t). \tag{3}$$

The presented assumption states that the total energy stored in $\mathcal{S}_i$ is equal to a function of the local states and its variation over time depends on $\mathcal{S}_i$'s power balance. This assumption is commonly valid in energy systems, as shown in [10]. For instance, the energy stored in a district heating network is a function of the water temperature, while in a power system it depends on the batteries' states of charge. For the sake of clarity, efficiencies related to power exchanges among different energy vectors are not considered in (3), but they can be easily included.

III. Control problem formulation

As discussed in Section I, the control of MES has to satisfy multiple specifications, i.e., optimize the overall MES $\mathcal{S}^\dagger$, optimize each subsystems $\mathcal{S}_i,\ \forall i \in \mathcal{N}$, and satisfy operative constraints. An effective MESs' control scheme must also deal with three main challenges: control architecture scalability, control actions at different time rates given the energy dynamics diversity, and involved energy distributors' privacy concerns. The proposed solution involves a two-layer control architecture, with a distributed coordination scheme at the high-level and a decentralized predictive control architecture at the low level. This distributed multi-layer control architecture main functioning is described hereafter with reference to Figure 1.

The subsystems' set $\mathcal{S}^\dagger$ is highlighted in grey. Each $\mathcal{S}_i$ has its own local low-level controller named Local-MPC$_i$ highlighted in green in Figure 1. Each L-MPC$_i$ runs at a time rate that suits $\mathcal{S}_i$'s dynamical behaviour and considers the nonlinear model (1). The local controller optimizes its

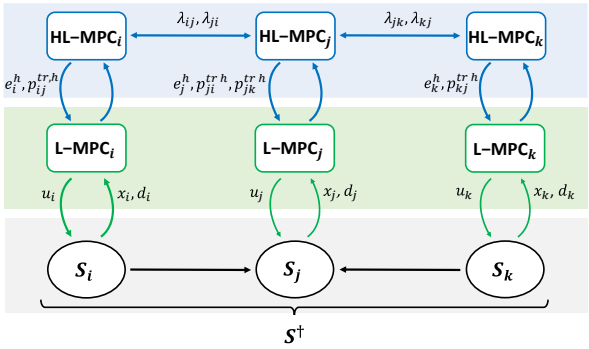

Fig. 1: Schematic of the MES distributed hierarchical control.

subsystem with two main goals: operational costs minimization and optimal references tracking of the total energy stored e_i^{h*} and power exchanges $p_{ij}^{tr\,h*}$ coming from the high-level layer, highlighted in blue in Figure 1. This layer consists of distributed predictive regulators named High-Level MPC$_i$ (HL-MPC$_i$) which optimize $\mathcal{S}_i$'s energy stored and power exchanges. Additionally, the HL-MPC$_i$ implements the reduced energy model (3) for its convexity that guarantees distributed algorithms' convergence and feasibility. Specifically, the high-level exploits the Dual Consensus ADMM (DC-ADMM) algorithm [11] for its enhance scalability and optimality performances.

Before describing the presented control architecture, define the L-MPC$_i$ sampling time as τ_i, its prediction horizon as $\mathcal{T}_i = \{k_i, \dots, k_i + N_i - 1\}$, where N_i are the prediction steps, while the current step is $k_i \in \mathbb{N}$, so $t = k_i \tau_i$. Furthermore, the sampling time of each HL-MPC$_i$ is τ_h, its prediction horizon is $\mathcal{T}_h = \{k_h, \dots, k_h + N_h - 1\}$, where N_h are the prediction steps, while the current step is $k_h \in \mathbb{N}$, hence $t = k_h \tau_h$. To simplify the notation, assume τ_h and τ_i to be multiples with $\tau_h = H_i \tau_i$ and $\tau_h \geq \tau_i \ \forall i \in \mathcal{N}$. Finally, assuming a suitable integration method, the nonlinear model (1a) becomes

$$\dot{x}_i(k+1) = \tilde{f}_i^s(x_i(k), u_i(k), \tilde{d}_i(k)), \tag{4}$$

where $\tilde{f}_i^s$ derives from the discretization of the continuous time state function f_i^s. In the same way, the discretized reduced energy model (3) is

$$e_i^h(k+1) = e_i^h(k) + \tau_h \left(p_i^{gh}(k) - p_i^{lh}(k) - \sum_{j \in \mathcal{N}_i} p_{ij}^{tr\,h}(k) \right). \tag{5}$$

A. Local MPC problem formulation

The general L-MPC$_i$ optimization problem is

$$\min_{u_i(\cdot), \sigma_i(\cdot)} \sum_{\forall k \in \mathcal{T}_i} \left(c_i^g p_i^g(k) + \alpha_i \sigma_i(k) \right) \tag{6a}$$

subject $\forall k \in \mathcal{T}_i$, to(4) and

$$\underline{x}_i \leq x_i(k) \leq \bar{x}_i, \tag{6b}$$
$$\underline{u}_i \leq u_i(k) \leq \bar{u}_i, \tag{6c}$$
$$p_i^g(k) = \phi_i(x_i(k), u_i(k)), \tag{6d}$$
$$\underline{p}_i^g \leq p_i^g(k) \leq \bar{p}_i^g, \tag{6e}$$
$$e_i(k) = \xi_i(x_i(k)), \tag{6f}$$
$$e_i(k) \leq e_i^{h*}\left(\left\lfloor \frac{k}{H_i} \right\rfloor | k_h \right) + \sigma_i(k) \tag{6g}$$
$$e_i(k) \geq e_i^{h*}\left(\left\lfloor \frac{k}{H_i} \right\rfloor | k_h \right) - \sigma_i(k) \tag{6h}$$
$$p_{ij}^{tr}(k) = p_{ij}^{tr\,h*}\left(\left\lfloor \frac{k}{H_i} \right\rfloor | k_h \right) \quad \forall j \in \mathcal{N}_i \tag{6i}$$
$$\sigma_i(k) \geq 0 \tag{6j}$$

The two terms of the L-MPC$_i$ cost function (6a) are the local power production cost $c_i^g \in \mathbb{R}_{\geq 0}^{g_i}$ and the minimization of the slack variable $\sigma_i \in \mathbb{R}_{\geq 0}$, where α_i is an arbitrary weight and $\alpha_i \gg max(c_i^g)$. The slack variable ensures the optimal high-level energy reference tracking feasibility. Energy and power reference tracking are enforced by constraints (6f) - (6i), where given the time rate of the high-level τ_h, $k_h = \lfloor (k_i / H_i) \rfloor$, $\forall i \in \mathcal{N}$. Recall that the optimal references e_i^{h*} and $p_{ij}^{tr\,h*}$ comes from the HL-MPC$_i$.

B. High level MPC problem formulation and distributed resolution

For the sake of clarity, we firstly present the centralized optimization problem and distribute it afterwards. Denote with $p_i^{gh}(k_h)$, $p_i^{lh}(k_h) \in \mathbb{R}$ the the high level generated and absorbed power at time k_h respectively. Hence, the centralized high level problem is

$$\min_{p_i^{gh}(\cdot), p_{ij}^{tr\,h}(\cdot)} \sum_{\forall i \in \mathcal{N}} \sum_{\forall k \in \mathcal{T}_h} \left(c_i^{gh}\, p_i^{gh}(k) + \sum_{j \in \mathcal{N}_i} \gamma_i^{tr} p_{ij}^{tr\,h}(k)^2 \right) + \sum_{\forall i \in \mathcal{N}} \beta_i (e_i^h(k_h + N_h) - e_i^{h0})^2 \tag{7a}$$

subject $\forall i \in \mathcal{N}$, $\forall k \in \mathcal{T}_h$, to (5),

$$\underline{e}_i^h \leq e_i^h(k) \leq \bar{e}_i^h, \tag{7b}$$
$$\underline{p}_i^{gh} \leq p_i^{gh}(k) \leq \bar{p}_i^{gh}, \tag{7c}$$
$$\underline{p}_i^{lh} \leq p_i^{lh}(k) \leq \bar{p}_i^{lh}, \tag{7d}$$
$$\underline{p}_{ij}^{tr\,h} \leq p_{ij}^{tr\,h}(k) \leq \bar{p}_{ij}^{tr\,h} \quad \forall j \in \mathcal{N}_i, \tag{7e}$$
$$e_i^h(k_h) = \tilde{e}_i^h(k_h), \tag{7f}$$
$$p_{ij}^{tr\,h}(k) + p_{ji}^{tr\,h}(k) = 0 \quad \forall j \in \mathcal{N}_i. \tag{7g}$$

In the centralized problem (7), upper and lower bounds (7b)-(7e) on the states and the generation cost c_i^{gh} in the cost function (7a) come from a proper aggregation of lower-level local variables, more details in [10]. Constraints (7f) initialize the total energy stored to the i-th subsystems' current energy state, where $\tilde{e}_i^h(k_h)$ is the total stored energy computed by the L-MPC at time instant k_h. Finally, we guarantee the power exchanges feasibility imposing the reciprocity constraints (7g). Concerning the cost function (7a), the first term is the local generation cost, the second one is the trading interface's usage cost, and the third is a terminal cost to avoid unnecessary usage of internal energy. Also, notice that thanks to the energy model, the resulting centralized problem (7) is convex. Although the presented formulation (7) is complete, a more compact representation is introduced to better describe its distributed resolution. For each $\mathcal{S}_i$, define the time step trading variable vector as $\boldsymbol{p}_i^{tr\,h}(k) = \{p_{ij}^{tr\,h}(k)\}_{\forall j \in \mathcal{N}_i}$ where $\boldsymbol{p}_i^{tr\,h}(k) \in \mathbb{R}^{M-1}$. Then, collect them in a single vector $\boldsymbol{p}_i^{tr\,h} = \{\boldsymbol{p}_i^{tr\,h}(k)\}_{k=k_h,\dots,k_h+N_h-1} \in \mathbb{R}^{(M-1)N_h}$. In analogy, define $\boldsymbol{e}_i^h = \{e_i^h(k)\}_{k=k_h,\dots,k_h+N_h} \in \mathbb{R}^{N_h+1}$ and

$\boldsymbol{p}_i^{gh} = \{p_i^{gh}(k)\}_{k=k_h,\dots,k_h+N_h-1} \in \mathbb{R}^{N_h}$ collecting variables influencing only subsystem i. The subsystems' optimization variables vector becomes

$$\boldsymbol{x}_i^h = \begin{bmatrix} \boldsymbol{e}_i^h \\ \boldsymbol{p}_i^{gh} \\ \boldsymbol{p}_i^{tr\,h} \end{bmatrix} \in \mathbb{R}^{x_i^h}. \tag{8}$$

Also, define the cost function of each agent $f_i(\boldsymbol{x}_i^h)$ as

$$f_i(\boldsymbol{x}_i^h) = \sum_{\forall k \in \mathcal{T}_h} \left(c_i^{gh}\, p_i^{gh}(k) + \sum_{j \in \mathcal{N}_i} \gamma_i^{tr} p_{ij}^h(k)^2 \right) + \beta_i (e_i^h(k_h + N_h) - e_i^{h0})^2.$$

Therefore, the centralized cost function (7a) becomes

$$\sum_{\forall i \in \mathcal{N}} f_i(\boldsymbol{x}_i^h). \tag{9}$$

Similarly, define the local constraint set $\mathcal{X}_i$ containing (5)-(7f), they are compactly written as

$$\boldsymbol{x}_i^h \in \mathcal{X}_i. \tag{10}$$

The reciprocity constraints (7g) can be compactly written as

$$\sum_{\forall i \in \mathcal{N}} \tilde{E}_i\, \boldsymbol{x}_i^h = \mathbb{0} \tag{11}$$

where the matrix $\tilde{E}_i = [\mathbb{0}\; blkdiag(\{E_i\}_{N_h})] \in \mathbb{R}^{(M-1)N_h,\, x_i^h}$ and each $E_i \in \mathbb{R}^{M-1, M-1}$ is defined as

$$[E_i]_{j,j} = \begin{cases} 1 & \text{if } (j \in \mathcal{N}_i \wedge j < i) \vee \\ & (j+1 \in \mathcal{N}_i \wedge j+1 > i), \\ 0 & \text{otherwise.} \end{cases} \tag{12}$$

for $j \in \{1, \dots, M-1\}$. Despite the definition of E_i in (12) is not intuitive, it enables the reciprocity constraint expression simplification from (7g) to (11) selecting the exchanged powers between subsystem $\mathcal{S}_i$ and its neighbours in $\mathcal{N}_i$.

In conclusion, the compact form of the centralized problem (13) is

$$\min_{\boldsymbol{x}_i^h(\cdot)} \sum_{\forall i \in \mathcal{N}} f_i(\boldsymbol{x}_i^h) \tag{13a}$$

s.t.

$$\boldsymbol{x}_i^h \in \mathcal{X}_i,\ \forall i \in \mathcal{N} \tag{13b}$$

$$\sum_{\forall i \in \mathcal{N}} \tilde{E}_i\, \boldsymbol{x}_i^h = \mathbb{0} \tag{13c}$$

We denote as *primal problem* this optimization problem, noting that it is convex. The DC-ADMM algorithm allows direct communication among agents and relies on iterative solutions that asymptotically converge to the centralized optimal value [13], [11], [16] in case of connected communication and convex problem. As problem (13) is already convex, to guarantee connected communications assume that each agent is able to communicate with at least one other agent. This assumption is reasonable as no isolated system would participate in a MES. The first step to implement the DC-ADMM algorithm is the construction of the Lagrangian function of problem (13) as

$$L(\boldsymbol{x}_1^h, \dots, \boldsymbol{x}_M^h) = \sum_{\forall i \in \mathcal{N}} \left(f_i(\boldsymbol{x}_i^h) + \boldsymbol{\lambda}\, \tilde{E}_i\, \boldsymbol{x}_i^h \right) \tag{14}$$

which is the relaxation of the reciprocity constraints (13c) with the introduction of the global dual variable $\boldsymbol{\lambda} \in \mathbb{R}^{(M-1)N_h}$. Based on the Lagrangian, we can define the *dual problem* as

$$\min_{\boldsymbol{\lambda}} \sum_{\forall i \in \mathcal{N}} \left(- \min_{\boldsymbol{x}_i^h \in \mathcal{X}_i} \left(f_i(\boldsymbol{x}_i^h) + \boldsymbol{\lambda}'\, \tilde{E}_i\, \boldsymbol{x}_i^h \right) \right) = \min_{\boldsymbol{\lambda}} \sum_{\forall i \in \mathcal{N}} \phi_i(\boldsymbol{\lambda}). \tag{15}$$

With the given assumptions, define $\boldsymbol{\lambda}_i$ the dual variable local copy for each subsystem i. It holds the equivalence between (15) and

$$\min_{\boldsymbol{\lambda}_1, \dots, \boldsymbol{\lambda}_M} \sum_{\forall i \in \mathcal{N}} \phi_i(\boldsymbol{\lambda}_i) \tag{16a}$$

$$\text{subject to } \boldsymbol{\lambda}_i = \boldsymbol{\lambda}_j \quad \forall i \in \mathcal{N},\ \forall j \in \mathcal{N}_i. \tag{16b}$$

Finally, the dual problem formulation (16) is separable and we can apply a standard consensus ADMM to solve it. The DC-ADMM algorithm implementation is reported for clarity in the following, where the superscript (k) indicates the ADMM iteration.

Algorithm 1 DC-ADMM

1: **Choose** $c > 0$. ▷ *Tuning parameter*
2: **Set** $\boldsymbol{x}_i^{h,0}$, $\boldsymbol{\lambda}i^0 = 0$, $\boldsymbol{\mu}_i^0 = 0 \quad \forall i \in \mathcal{N}$.
3: $k \leftarrow 1$. ▷ *ADMM Iteration counter*
4: **repeat**
5: **for all** $i \in \mathcal{N}$ **do** ▷ *Each agent in parallel*
6: $\boldsymbol{\mu}_i^{(k)} = \boldsymbol{\mu}_i^{(k-1)} + c \sum_{j \in \mathcal{N}_i} \left(\boldsymbol{\lambda}_i^{(k-1)} - \boldsymbol{\lambda}_j^{(k-1)} \right),$
7: $\boldsymbol{x}_i^{h,(k+1)} = \underset{\boldsymbol{x}_i^h \in \mathcal{X}_i}{\operatorname{argmin}} \left(f_i(\boldsymbol{x}_i^h) + \right.$
$\left. + \frac{c}{4n_i} \left\| \frac{\tilde{E}_i \boldsymbol{x}_i^h - \boldsymbol{\mu}_i^{(k)}}{c} + \sum_{j \in \mathcal{N}_i} \left(\boldsymbol{\lambda}_i^{(k-1)} - \boldsymbol{\lambda}_j^{(k-1)} \right) \right\|^2 \right),$
8: $\boldsymbol{\lambda}_i^{(k)} = \frac{1}{2n_i} \left(\sum_{j \in \mathcal{N}_i} \left(\boldsymbol{\lambda}_i^{(k-1)} - \boldsymbol{\lambda}_j^{(k-1)} \right) \right.$
$\left. - \boldsymbol{\mu}_i^{(k)}/c + \tilde{E}_i \boldsymbol{x}_i^{h(k+1)}/c \right).$
9: Share $\boldsymbol{\lambda}_i^k$ with $\forall j \in \mathcal{N}_i$
10: $k \leftarrow k+1$
11: **until** Tolerances are met

In Algorithm 1, we can see the computational effort, Steps 6-9, is pushed down to the agents and the solution is parallelized. Moreover, the goal of distribution is reached thanks to the communication Step 9, where agents interact with neighbours and exchange dual informations. At each iteration, the agents locally update $\boldsymbol{\lambda}_i$ (Step 8), their optimal solution (Step 7) and the dual variable $\boldsymbol{\mu}_i$ (Step 6). The dual variables $\boldsymbol{\mu}$ guarantee the convergence of the variables $\boldsymbol{\lambda}$ to the same value. In turn, $\boldsymbol{\lambda}$'s convergence ensures the dual problem solution feasibility.

IV. Numerical example

In this section, we investigate the performance of the distributed two-layer control architecture applied to a multi-

energy case study reported in Figure 2 and composed of three interconnected energy subsystems of different domains: a H_2 energy system (depicted in dark blue), a thermal network (with supply pipelines depicted in red and return ones in light blue), and a electricity grid (depicted in green). The electricity grid is based on the IEEE 37-bus system [17] and the district heating network on the AROMA network described in [15]. The main parameters of the energy subsystems and their units are reported in Table I. The results relate to a 24h MES optimization where the control parameters are also in Table I, and the nondispatchable profiles are reported in Figure 3 together with power costs. The IEEE 37-bus systems uses the power flow model to simulate the behaviour of its elements, while the gas system equations are presented in [10]. Lastly, the AROMA network simulation runs in Simscape and its models are based on standard nonlinear thermo-hydraulic equations as in [15]. The HL-MPC layer is implemented with a prediction horizon of 24 hours and a time-rate of $\tau_h = 30$ min. This is solved relying on the DC-ADMM procedure reported in Algorithm 1, where parameter $c = 1e^{-2}$. The convergence tolerance of the dual variables is $1e^{-4}$, and the ADMM cycle takes, on average, $127\,s$ when executed sequentially. The parallelization of the computation would significantly drop the ADMM cycle computational time. In this paper, to keep the explanation concise, only one dual variable appears.

We use the hierarchical control structure of Figure 1 to optimize one day of operation and obtained the results reported in Figure 4. Some results are normalized with respect to their maximum value to display different energy vectors jointly. The cost of electricity varies during the day. Since it is the pivotal driver of the HL-MPC economical optimization, the subsystems' total energy stored references and power generation profiles reflect the cost variation, as in Figure 4. In particular, the MES HL-MPC profiles proves the effectiveness of the coordination in Figures 4a-4c. The three subsystems work together to indirectly store electricity as hydrogen or heat when most convenient and deliver it back later when energy prices rise. Moreover, we can notice the limitation of different forms of energy in Figure 4a. The battery profile (green) is the fastest-changing as batteries are fast to charge and discharge, whereas the thermal energy (red) has the slowest delivery time. Additionally, consider the energy trading between $\mathcal{S}_1$ and $\mathcal{S}_2$ in Figure 4b. Since the heat pump is more efficient than the gas boiler, it runs all day according to electrical energy availability, specifically at night and in the afternoon, when loads absorb the least and solar production is highest, respectively. Now, consider the energy trading between $\mathcal{S}_1$ and $\mathcal{S}_3$ in Figure 4c. The hydrogen energy system can store and produce electricity thanks to an electrolyzer and a fuel cell. These components activate during one day of operation. Specifically, hydrogen is produced during electricity low-cost hours, i.e., early in the morning and at midday, and consumed to produce electricity at peak cost hours.

Figure 4a reports the profiles of the normalized energy references dictated by the high-level layer, where energy is stored when most convenient. The L-MPC regulators track the energy references as shown in Figures 4d-4f. Specifically, the $\mathcal{S}_1$ batteries' states of charge are depicted in Figure 4d, the $\mathcal{S}_3$ gas density is shown in Figure 4f, whereas Figure 4e illustrates the $\mathcal{S}_2$ pipe temperatures. The latter shows how the L-MPC$_2$ regulator allows to store energy in pipelines, a strategy known as packing [18] in thermal energy control.

$\mathcal{S}_i$	$\mathcal{S}_1$	$\mathcal{S}_2$	$\mathcal{S}_3$
τ_i min	1	30	5
$\mathcal{T}_i$ hours	24	24	24
$(\underline{e}_i^{h0}, \bar{e}_i^{h})$ kWh	50	$10.4e^3$	25.4
$(\underline{e}_i^{h}, \bar{e}_i^{h})$ kWh	(10, 90)	$(9.4, 12)e^3$	(3.5, 50.2)
$(\underline{p}_i^{gh}, \bar{p}_i^{gh})$ kW	$(-500, 500)$	(0, 700)	(0, 78.5)
$(\underline{p}_{i1}^{tr\,h}, \bar{p}_{i1}^{tr\,h})$ kW	–	$(-200, 0)$	$(-250, 250)$
$(\underline{p}_{i2}^{tr\,h}, \bar{p}_{i2}^{tr\,h})$ kW	(0, 200)	–	–
$(\underline{p}_{i3}^{tr\,h}, \bar{p}_{i2}^{tr\,h})$ kW	$(-250, 250)$	–	–

TABLE I: Control parameters of the case study.

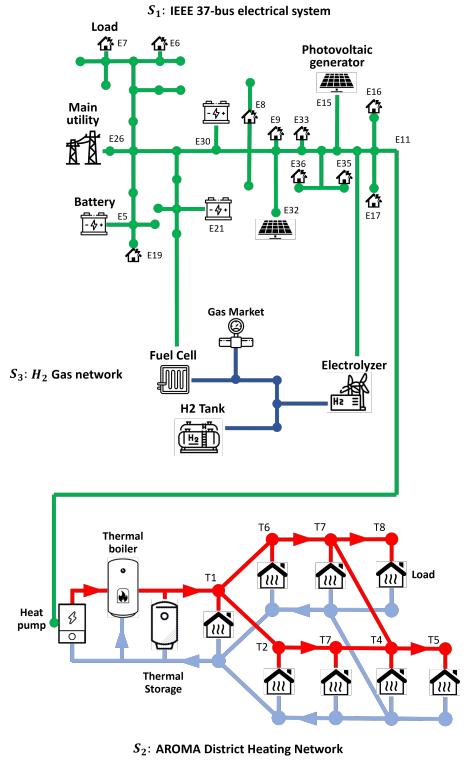

Fig. 2: Topology of the numerical example network.

V. CONCLUSIONS

In conclusion, the proposed two-layer distributed control architecture for MES systems solves the issues of scalability and time rates diversity. This results are possible through a decentralized framework of MPC regulators at the low level, locally controlling each energy vector with its detailed modelling, and a high-level layer of distributed MPC systems, coordinating MES subsystems. The application of a distributed algorithm is made possible thanks to a novel convex unified energy modelling. The results showed promising performances when tested on the large networks presented in

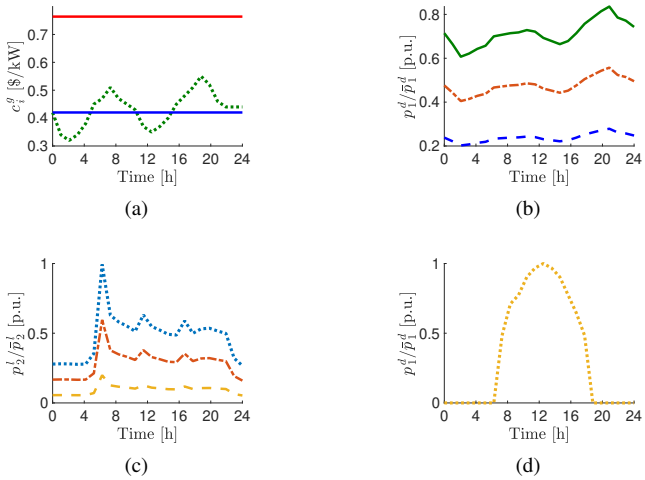

Fig. 3: (a) Power generation costs: c_1^g in green, c_2^g in red, c_3^g in blue. (b) Normalized electrical loads. (c) Normalized thermal loads. (d) Normalized solar panel production.

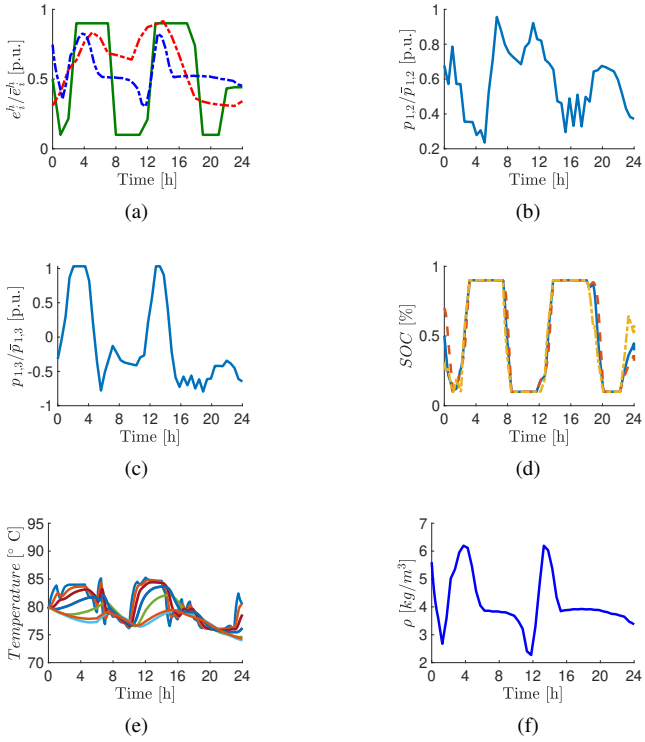

Fig. 4: (a) Normalized energy storage of systems $\mathcal{S}_1$ (green), $\mathcal{S}_2$ (red), and $\mathcal{S}_3$ (blue). (b) Normalized energy exchange between $\mathcal{S}_1$ and $\mathcal{S}_2$. (c) Normalized energy exchange between $\mathcal{S}_1$ and $\mathcal{S}_3$. (d) Batteries' state of charge. (e) Temperature of the water in pipes. (f) Gas density inside the H_2 storage.

the case study. Future work will focus on the development of game-theoretical coordination schemes for multi-energy systems, enabling negotiation mechanisms among operators of different energy vectors, so as to agree the optimal multi-energy power exchanges.

ACKNOWLEDGMENT

The research activity of Lorenzo Nigro has been financed by the Research Fund for the Italian Electrical System under the Contract Agreement between RSE S.p.A. and the Ministry of Economic Development - General Directorate for the Electricity Market, Renewable Energy and Energy Efficiency, Nuclear Energy in compliance with the Decree of April 16th, 2018. The work of Riccardo Scattolini is carried out within the MICS (Made in Italy – Circular and Sustainable) Extended Partnership and received funding from Next-Generation EU (Italian PNRR – M4 C2, Invest 1.3 – D.D. 1551.11-10-2022, PE00000004). CUP MICS D43C22003120001.

REFERENCES

[1] G. Chicco, S. Riaz, A. Mazza, and P. Mancarella, "Flexibility from distributed multienergy systems," *Proceedings of the IEEE*, vol. 108, no. 9, pp. 1496–1517, 2020.

[2] C. Klemm and P. Vennemann, "Modeling and optimization of multi-energy systems in mixed-use districts: A review of existing methods and approaches," *Renewable and Sustainable Energy Reviews*, vol. 135, p. 110206, 2021.

[3] P. Mancarella, "Mes (multi-energy systems): An overview of concepts and evaluation models," *Energy*, vol. 65, pp. 1–17, 2014.

[4] M. Arnold, R. R. Negenborn, G. Andersson, and B. De Schutter, "Model-based predictive control applied to multi-carrier energy systems," in *2009 IEEE power & energy society general meeting*. IEEE, 2009, pp. 1–8.

[5] S. Long, O. Marjanovic, and A. Parisio, "Generalised control-oriented modelling framework for multi-energy systems," *Applied Energy*, vol. 235, pp. 320–331, 2019.

[6] A. Lesage-Landry, H. Wang, I. Shames, P. Mancarella, and J. A. Taylor, "Online convex optimization of multi-energy building-to-grid ancillary services," *IEEE Transactions on Control Systems Technology*, vol. 28, no. 6, pp. 2416–2431, 2019.

[7] A. La Bella, A. Del Corno, and A. Scaburri, "Data-driven modelling and optimal management of district heating networks," in *2021 AEIT International Annual Conference (AEIT)*. IEEE, 2021, pp. 1–6.

[8] G. Ceusters, R. C. Rodríguez, A. B. García, R. Franke, G. Deconinck, L. Helsen, A. Nowé, M. Messagie, and L. R. Camargo, "Model-predictive control and reinforcement learning in multi-energy system case studies," *Applied Energy*, vol. 303, p. 117634, 2021.

[9] A. La Bella, F. Bonassi, M. Farina, and R. Scattolini, "Two-layer model predictive control of systems with independent dynamics and shared control resources," *IFAC-PapersOnLine*, vol. 52, no. 3, pp. 96–101, 2019.

[10] A. La Bella, L. Nigro, and R. Scattolini, "Predictive control and benefit sharing in multi-energy systems," *IEEE Transactions on Control Systems Technology*, 2023.

[11] T.-H. Chang, M. Hong, and X. Wang, "Multi-agent distributed optimization via inexact consensus admm," *IEEE Transactions on Signal Processing*, vol. 63, no. 2, pp. 482–497, 2014.

[12] A. La Bella, A. Falsone, D. Ioli, M. Prandini, and R. Scattolini, "A mixed-integer distributed approach to prosumers aggregation for providing balancing services," *International Journal of Electrical Power & Energy Systems*, vol. 133, p. 107228, 2021.

[13] V. N. Behrunani, A. Irvine, G. Belgioioso, P. Heer, J. Lygeros, and F. Dörfler, "Designing fairness in autonomous peer-to-peer energy trading," *IFAC-PapersOnLine*, vol. 56, no. 2, pp. 3751–3756, 2023.

[14] A. La Bella, P. Klaus, G. Ferrari-Trecate, and R. Scattolini, "Supervised model predictive control of large-scale electricity networks via clustering methods," *Optimal Control Applications and Methods*, vol. 43, no. 1, pp. 44–64, 2022.

[15] R. Krug, V. Mehrmann, and M. Schmidt, "Nonlinear optimization of district heating networks," *Optimization and Engineering*, vol. 22, pp. 783–819, 2021.

[16] G. Banjac, F. Rey, P. Goulart, and J. Lygeros, "Decentralized resource allocation via dual consensus admm," in *2019 American Control Conference (ACC)*. IEEE, 2019, pp. 2789–2794.

[17] W. H. Kersting, "Radial distribution test feeders," in *2001 IEEE Power Engineering Society Winter Meeting. Conference Proceedings (Cat. No. 01CH37194)*, vol. 2. IEEE, 2001, pp. 908–912.

[18] L. Saarinen, "Modelling and control of a district heating system," 2008.